

# Constrained Submodular Optimization for Vaccine Design

Zheng Dai<sup>1</sup>[0000-0002-8828-1075] and David K. Gifford<sup>1</sup>[0000-0003-1709-4034]

Computer Science and Artificial Intelligence Laboratory, Massachusetts Institute of Technology, Cambridge MA  
02139, USA

{zhengdai,gifford}@mit.edu

**Abstract.** Advances in machine learning have enabled the prediction of immune system responses to prophylactic and therapeutic vaccines. However, the engineering task of designing vaccines remains a challenge. In particular, the genetic variability of the human immune system makes it difficult to design peptide vaccines that provide widespread immunity in vaccinated populations. We introduce a framework for evaluating and designing peptide vaccines that uses probabilistic machine learning models, and demonstrate its ability to produce designs for a SARS-CoV-2 vaccine that outperform previous designs. We provide a theoretical analysis of the approximability, scalability, and complexity of our framework.

**Keywords:** Immunology · Vaccine · Computational biology · Submodular optimization.

## 1 Introduction

Peptide vaccines that expand and activate T cells have emerged as a promising prophylactic and therapeutic approach for addressing health related challenges including infectious diseases and cancer [7]. In contrast to more conventional live-attenuated vaccines that are based on entire organisms, or subunit vaccines that are based on entire protein subunits, peptide vaccines are based on a small set of protein fragments (peptides) that are sufficient to induce a T cell immune response, enabling the elicitation of far more targeted responses that avoid allergenic and reactogenic responses [5].

The design of a peptide vaccine consists of selecting immunogenic protein fragments, usually referred to as epitopes [5], that when included in a vaccine expand epitope specific T cells. Advances in machine learning has enabled our ability to predict which peptides will be presented by major histocompatibility complex (MHC) molecules for surveillance by the adaptive immune system [1, 12], which can be used to identify which epitopes will be displayed [13].

The epitopes displayed by an individual depend upon the specific alleles of their MHC genes, and thus the peptides displayed by the immune system can vary greatly from individual to individual [14]. Therefore, the engineering task of finding a set of peptides that is predicted to be displayed by a large portion of the population remains challenging despite progress on the peptide-MHC display task.

In this work we introduce a framework for evaluating and designing peptide vaccines that uses probabilistic interpretations of machine learning models, and demonstrate its ability to produce designs for the SARS-CoV-2 vaccine design task that outperform previous designs. We complement this with a theoretical analysis of the approximability, scalability, and complexity of our framework, which may be of independent interest.

### 1.1 Contributions

To improve the effectiveness of a vaccine it is important to introduce redundancies into its design so the failure of a single displayed peptide to elicit an immune response does not become a single point of failure [6]. Vaccines designed with an  $n$ -times coverage objective aim to obtain at least  $n$  immunogenic peptide “hits” in each person. Having more than one “hit” provides redundancy to expand multiple T cell clonotypes in an individual to fight disease, protects against peptide sequence drift as a consequence of pathogen or tumor mutations, protects against the loss of an MHC gene, and accounts for the variability of peptide immunogenicity between individuals.

We show that optimizing the population coverage for strict  $n$ -times coverage guarantees cannot be tractably approximated to any constant factor assuming the intractability of the GAP-SMALL-SET EXPANSION

problem [11], which may be of independent interest. Here we propose an alternative framework that uses a soft redundancy guarantee as its objective. The resulting objective is both submodular and monotonic, and can therefore be approximated via a greedy approach. Our proposed framework also has additional desirable properties: it makes explicit the utility of the redundancy, does not discount the benefits of being covered without redundancy, and is able to reason with uncertainty when working with machine learning based predictions.

While redundancies in a design are important, it is also important that they be *dissimilar redundancies*, since reasons for failure may be shared between similar peptides. This additional constraint that selected peptides be dissimilar is highly problematic as it allows the problem formulation to encode an NP-hard problem that in the general case can not be approximated to any constant factor. However, by parameterizing on the structure of the constraints, we can derive lower bounds for the performance of the greedy approach which show that the greedy approach can still provide approximation guarantees in situations of interest. These bounds may also be of independent interest.

## 1.2 Related work

The use of computational methods to aid vaccine design has taken on an increasingly important role in the vaccine design process over the past two decades [8]. Much of the advancement stems from improvements in the epitope identification task, which has seen great improvement with advances in data collection strategies and machine learning [1, 12]. While good epitope prediction tools are essential to vaccine design, the focus of this work is on the downstream task of selecting defined epitopes for vaccine inclusion.

Earlier work on vaccine design are reviewed in Oyarzun and Kobe [10], and employ discrete optimization techniques such as integer linear programming and genetic algorithms to optimize population coverage. However, they do not anticipate or solve the problem of coverage with dissimilar redundancies [6], which we do in this work. Furthermore, they do not consider the epistemic uncertainty associated with epitope predictions, which we do.

Our work is closely related to the work in [6], where the use of an objective that accounts for dissimilar redundancies is proposed. However, approximating their proposed objective to any constant factor appears to be an intractable problem, while our objective permits constant factor approximations in polynomial time. Our framework also allows for reasoning about redundancies with uncertainty, which theirs does not for more than 1-times coverage.

## 1.3 Presentation

In the remaining four sections of the paper we present the optimization problem that we wish to solve (Section 2), provide an algorithm for solving the problem and analyze its runtime and approximation guarantees (Section 3), apply our framework to the SARS-CoV-2 vaccine design problem (Section 4), and conclude with a discussion (Section 5). Theorems are presented where appropriate throughout, while proofs are relegated to Appendix A for improved flow.

## 2 A diminishing returns objective provides a submodular solution

Peptide vaccines are designed by considering the peptide sequence(s) of a target of interest, for example the proteome of a virus, and selecting a small set of peptides within the target sequences to include in the vaccine. Vaccine peptides are selected such that they elicit an immune response in a large portion of a susceptible population we wish to vaccinate. This is done by selecting vaccine peptides that are displayed on the cell surface by MHC proteins. The resulting peptide-MHC complexes activate the cellular immune system. The challenge of selecting a set of peptides arises from the polymorphism present in MHCs. Different MHC alleles have different peptide binding properties, so the peptides must be carefully chosen in order to elicit widespread immune responses from a given population.

## 2.1 Preliminaries

Let  $\mathbb{R}^{\geq 0}$  denote non-negative real numbers. Let  $E$  be some finite set of elements. Let  $F : 2^E \rightarrow \mathbb{R}^{\geq 0}$ . We say  $F$  is submodular if  $F(S_1 \cup \{e\}) - F(S_1) \geq F(S_2 \cup \{e\}) - F(S_2)$  whenever  $S_1 \subseteq S_2$  and  $e \in E$ , and we say that  $F$  is monotonically increasing if  $S_1 \subseteq S_2 \implies F(S_1) \leq F(S_2)$  for all  $S_1, S_2 \subseteq E$ .

Suppose  $G = (V, E)$  is a graph. For simplicity, we will at times use  $G_V$  to denote the vertex set  $V$  and  $G_E$  to denote the edge set  $E$ . The  $k$ th power of  $G$ , denoted  $G^k$ , is defined as the graph  $(G_V^k, G_E^k)$ , where  $G_V^k = G_V$  and  $G_E^k$  contains all pairs of vertices between which there exists a path of length less than or equal to  $k$  in  $G$ .

We will use  $\mathbb{1}_X$  to denote an indicator that evaluates to 1 if  $X$  is true and 0 otherwise.

## 2.2 Optimizing population coverage with redundancies is computationally difficult

It is important for a vaccine to cause the display of multiple epitopes in individuals to provide redundancy in the activation of T cell clonotypes, to expand multiple T cell clonotypes in an individual to fight disease, to protect against peptide sequence drift as a consequence of pathogen or tumor mutations, to protect against the loss of an MHC gene, and to account for the variability of peptide immunogenicity between individuals [6]. In Liu et al. [6], the authors showed that previous vaccine designs fail to cover significant portions of the population when coverage criteria include these redundancies. To address this, they introduce the  $n$ -times coverage framework, which involves solving the max  $n$ -times coverage problem. The problem is defined as follows:

**Definition 1.** *Given a ground set, a set of weights over the ground set, a collection of multisets, and some cardinality constraint  $k$ , find a collection of  $k$  multisets such that the aggregate weights of the elements in the ground set that are covered at least  $n$  times is maximized.*

For vaccine design, the ground set corresponds to MHC genotypes, the weights correspond to the percentage of the population with the genotypes, and each multiset corresponds to a peptide, which covers certain genotypes a variable number of times. Solving this problem with cardinality constraint  $k$  then gives a vaccine design consisting of  $k$  peptides, with the objective that a large portion of the population display at least  $n$  peptides (i.e. have at least  $n$  peptide-MHC hits).

While this is a natural extension of earlier vaccine design paradigms that do not account for redundancies, it is a computationally difficult problem. The authors have shown in their work that this is an NP-hard optimization problem, and so they propose heuristic approaches. Here, we provide evidence suggesting that even finding some constant factor approximation cannot be achieved in polynomial time.

**Theorem 1.** *For any  $\epsilon > 0$ , if there exists a polynomial time algorithm that can achieve an approximation factor of  $\epsilon$  to max  $n$ -times coverage, then there exists a polynomial time algorithm that can decide GAP-SMALL-SET EXPANSION( $\eta$ ) for some  $\eta \in (0, 0.5)$ .*

There is currently no known polynomial time algorithm for GAP-SMALL-SET EXPANSION( $\eta$ ) for any  $\eta \in (0, 0.5)$ . The *Small Set Expansion Hypothesis* conjectures that GAP-SMALL-SET EXPANSION( $\eta$ ) is NP-hard for any  $\eta \in (0, 0.5)$ , and is currently an open problem related to the Unique Games Conjecture[11].

## 2.3 A diminishing returns framework for vaccine design provides a submodular optimization objective

A key reason underlying the complexity of the max  $n$ -times coverage problem is the utility of a peptide may be hidden until we are close to reaching  $n$ -times coverage. This makes it difficult select peptides optimally. To address this, we use a diminishing returns framework, where peptides will improve the objective at any coverage level. Intuitively, this provides a “gradient” along which an optimization procedure can climb.

Let  $U : \mathbb{R}^{\geq 0} \rightarrow \mathbb{R}^{\geq 0}$  be some non-negative monotonically increasing concave function such that  $U(0) = 0$ . Let  $\mathcal{M}$  denote the set of MHC genotypes observed in the population. Let  $w : \mathcal{M} \rightarrow \mathbb{R}^{\geq 0}$  be a weight function that gives the frequency of each genotype in the population. Let  $\mathcal{P}$  denote the set of candidate peptides where a subset is selected for vaccine design. If  $p \in \mathcal{P}$  and  $m \in \mathcal{M}$ , let  $display(p, m)$  denote the predicate

of whether  $p$  is displayed in an individual with genotype  $m$ . To model uncertainty, we let  $display(p, m)$  operate over the sample space of some probability distribution. The objective, parametrized by  $U$ , can then be written as follows:

$$\mathcal{F}_U(S) = \sum_{m \in \mathcal{M}} w(m) \mathbb{E}[U(\sum_{p \in S} \mathbb{1}_{display(p, m)})] \quad (1)$$

Where  $S \subseteq \mathcal{P}$  is the set of peptides selected for vaccine inclusion. This objective is a monotonically increasing submodular function.

**Theorem 2.** *For any  $U : \mathbb{R}^{\geq 0} \rightarrow \mathbb{R}^{\geq 0}$  that is monotonically increasing and concave,  $\mathcal{F}_U$  is a monotonically increasing submodular function.*

Beyond submodularity, this objective has several additional desirable properties: first, it accounts for the fact that having peptide-MHC hits is useful, even if the redundancy does not obtain a given threshold. While having high redundancy is better than having low redundancy, having low redundancy is better than not displaying any peptides. Second, this formulation makes explicit the utility we expect from attaining a given number of peptide-MHC hits, which is provided as  $U$ . Third, it allows reasoning with uncertainty by allowing  $display(p, m)$  to be an uncertain event. Many prediction models output a soft classification instead of a hard one, which we can calibrate to attach uncertainties to the classifications.

For an arbitrary distribution over the set of indicator variables  $\mathbb{1}_{display(p, m)}$ , we may need to approximate the expectation in  $\mathcal{F}_U$  via sampling. However, we can compute the objective  $\mathcal{F}_U$  exactly and efficiently if we suppose that for a given MHC genotype  $m$ , the set of indicator variables  $\mathbb{1}_{display(p, m)}$  are independent. This is almost certainly false given a sufficiently large pool of peptide sequences, since we should be able to significantly improve the performance of a predictor by training it on a sufficiently large number of peptide sequences. However, we can weaken this assumption to  $k$ -wise independence if we only consider vaccine designs that include at most  $k$  peptides. For values of  $k$  that are reasonable in the context of designing peptide vaccines, this assumption is more reasonable than the full independence assumption.

Under the independence assumption we can calculate the objective by computing the distribution of the sum via iterated convolutions of Bernoulli distributions, and then taking the expectation using the distribution (see Appendix C for additional details). This runs in time  $\mathcal{O}(|\mathcal{M}||S|^2)$ , where  $|\mathcal{M}|$  is the number of genotypes and  $|S|$  is the number of peptides in the vaccine design.

## 2.4 Peptide selections need to be constrained to avoid unreasonable designs

We impose two types of constraints on the set of peptides selected for vaccine inclusion: a cardinality constraint, and a set of pairwise constraints.

The cardinality constraint is necessary since our objective function is monotonically increasing. Therefore, the full set of candidate peptides  $\mathcal{P}$  will maximize it. This is undesirable, since peptide vaccines need to be compact to permit effective delivery and to induce effective intolerance in the context of limited immune system capacity. Therefore, we will impose a cardinality constraint on the set of selected peptides such that it cannot exceed a given size  $k$ .

The pairwise constraints are required to avoid very similar peptides from being included. Peptide candidates for vaccine inclusion are generated by sliding windows of various sizes across the protein sequence we wish to target. This produces peptides that are highly similar in sequence, such as nested sequences, and including highly related sequences does not truly improve the effectiveness of the vaccine. Furthermore, the assumption that the variables indicating peptide-MHC interactions are independent likely does not hold when peptides are very similar, since it is possible that the predictor makes use of similar features, which result in systematic errors. Therefore, we introduce a set of pairwise constraints  $\mathcal{G}$  as a graph where the vertex set  $\mathcal{G}_V = \mathcal{P}$ , and where edges exist between peptides that are deemed redundant. We then require that the peptides in the vaccine design form an independent set within  $\mathcal{G}$ .

### 3 Methods

#### 3.1 A greedy approach attains bounded performance under the diminishing returns framework

Our goal is the following: given a peptide set  $\mathcal{P}$ , a set of MHC genotypes  $\mathcal{M}$ , binding credences between all peptides and MHCs, a monotonically increasing concave utility function  $U : \mathbb{R}^{\geq 0} \rightarrow \mathbb{R}^{\geq 0}$  with  $U(0) = 0$ , a cardinality constraint  $k$ , and pairwise constraints  $\mathcal{G}$ , find a set  $S \subseteq \mathcal{P}$  that satisfies all the constraints and maximizes the objective function  $\mathcal{F}_U(S)$ .

We will use the greedy approach provided in Algorithm 1 to produce a solution to this problem. The procedure is straightforward: at each iteration we add the peptide that maximally improves the solution to the solution set, then eliminate that peptide and all similar peptides from consideration for all future steps.

---

**Algorithm 1:** Peptide set selection for the diminishing returns framework

---

**Input:** A ground set of candidate peptides  $\mathcal{P}$ , a cardinality constraint  $k$ , a similarity graph  $(\mathcal{P}, E)$ , and a monotone submodular function  $F : 2^{\mathcal{P}} \rightarrow \mathbb{R}^{\geq 0}$  where  $F(\emptyset) = 0$

**Result:** A set  $S \subseteq \mathcal{P}$  such that  $|S| \leq k$

$S \leftarrow \emptyset;$

$Q \leftarrow \mathcal{P};$

**while**  $(Q \neq \emptyset) \wedge (|S| < k)$  **do**

$x \leftarrow \arg \max_{x \in Q} F(S \cup \{x\});$   
 $S \leftarrow S \cup x;$   
 $N \leftarrow \{y | \{x, y\} \in E\} \cup \{x\};$   
 $Q \leftarrow Q \setminus N;$

**return**  $S;$

---

**Runtime analysis for Algorithm 1** Evaluating the objective function for each proposal takes time at most  $\mathcal{O}(k^2|\mathcal{M}|)$ , since the design itself will never contain more than  $k$  elements. To compute the arg max, the objective needs to be evaluated for every element in  $\mathcal{P}$  in the worst case. Removing peptides from consideration at the end of each iteration can be done in time  $\mathcal{O}(|\mathcal{P}|)$ . Overall,  $k$  iterations are performed, leading to an overall runtime of  $\mathcal{O}(k^3|\mathcal{P}||\mathcal{M}|)$ .

We optimize our computation of arg max by calculating the marginal improvement of a candidate peptide rather than the full vaccine score. Computing the marginal improvement can be done in time  $\mathcal{O}(k|\mathcal{M}|)$  rather than  $\mathcal{O}(k^2|\mathcal{M}|)$  (see Appendix C), attaining significant speedup. Second, scoring can be vectorized, allowing us to parallelize much of the computation (see Appendix C). Each iteration only requires  $\mathcal{O}(1)$  vector operations along with up to  $\mathcal{O}(|\mathcal{P}|)$  operations to remove peptides from consideration, so the overall computation only requires  $\mathcal{O}(k)$  vector operations and  $\mathcal{O}(|\mathcal{P}|k)$  other operations. It is still the case that  $\mathcal{O}(k^2|\mathcal{P}||\mathcal{M}|)$  operations need to be performed overall, and in practice  $|\mathcal{M}|$  and  $|\mathcal{P}|$  are sufficiently large that the vectorized operations need to be run in sequential batches, so those parameters still play a significant role in the runtime.

Our implementation can generate designs of size  $k \approx 10^2$  over a peptide set of size  $|\mathcal{P}| \approx 10^3$  with  $|\mathcal{M}| \approx 10^6$  genotypes in approximately 5 minutes when parallelized over 8 Titan RTX GPUs. See Appendix C for additional details.

**Approximation ratio of Algorithm 1** Let  $S^*$  denote the true optimum of the optimization problem. If we let each peptide and MHC genotype interact with probability 1 and let  $k$  be sufficiently large, then the desired optimization is equivalent to finding the maximum independent set within  $\mathcal{G}$ . Finding any constant factor approximation to max-clique is NP-hard [15], which then immediately implies that  $S^*$  cannot be approximated to any constant factor. Therefore, the quality of the solution produced by Algorithm 1 cannot be unconditionally bounded by a constant factor with respect to  $S^*$ , since Algorithm 1 runs in polynomial time.

However, we can bound the performance by looking at the graph structure of  $\mathcal{G}$ . Since we are considering cases where similarity relations are mostly generated from sliding windows over linear sequences, we might expect the resulting graph to be of low degree. Let  $\Delta(\mathcal{G})$  denote the degree of  $\mathcal{G}$ . Note that in the special case where  $\Delta(\mathcal{G}) = 0$ , there are no pairwise constraints, so the problem reduces to the optimization of a monotonic submodular function under a cardinality constraint. It is well established that the greedy approach attains an approximation ratio of  $(1 - e^{-1})$  in this case [9], and that attaining an approximation ratio of  $(1 - e^{-1} + \epsilon)$  for any  $\epsilon > 0$  is NP-hard[2].

Another property we can look at is the graph power of  $\mathcal{G}$ . We may expect that in the case where a graph looks like a path, taking the graph power would not add too many extra constraints, in which case replacing  $\mathcal{G}$  with its graph power  $\mathcal{G}^p$  would not yield a optimum that is too different. Let  $S_p^*$  denote the solutions to the more constrained optimizations:

$$S_p^* = \underset{\substack{S \subseteq \mathcal{P}: |S| \leq k \\ v_1, v_2 \in S \implies \{v_1, v_2\} \notin \mathcal{G}_E^p}}{\arg \max} \mathcal{F}_U(S) \quad (2)$$

We can then bound the output of Algorithm 1 by incorporating these extra graph parameters:

**Theorem 3.** *Let  $\hat{S}$  be the output of Algorithm 1. Then:*

1. If  $\Delta(\mathcal{G}) = 0$ , then  $\mathcal{F}_U(\hat{S}) \geq \mathcal{F}_U(S^*)(1 - e^{-1})$
2. If  $\Delta(\mathcal{G}) > 0$ , then  $\mathcal{F}_U(\hat{S}) \geq \max(\frac{\mathcal{F}_U(S_2^*)}{2}, \frac{\mathcal{F}_U(S^*)}{1 + \Delta(\mathcal{G})})$

We can upper bound the best possible performance of polynomial time algorithms.

**Theorem 4.** *Unless  $P = NP$ , there exists no polynomial time algorithm that can output an approximation  $\hat{S}$  that guarantees either of the following on all inputs for any  $\epsilon > 0$ :*

1.  $\mathcal{F}_U(\hat{S}) \geq \mathcal{F}_U(S_2^*)(1 - e^{-1} + \epsilon)$
2.  $\mathcal{F}_U(\hat{S}) \geq \mathcal{F}_U(S^*)(\frac{1}{1 + \Delta(\mathcal{G})})^{(1 - \epsilon)}$

### 3.2 Using neural network based models to attain binding credences

We define  $display(p, m)$  as a random event in a probability space of beliefs that peptide  $p$  is presented by MHC genotype  $m$ . We use the well established neural network based model NetMHCpan4.1 [12] to generate predictions that we use to derive  $\Pr(display(p, m))$ . We will assume that the derived beliefs are independent (although it is sufficient to assume  $k$ -wise independence, and only between events that share a genotype - see Section 2.3). While this may not necessarily be true for closely related sequences, we circumvent this by constraining our designs such that they do not contain closely related sequences (see Section 2.4).

We will focus on designing a peptide vaccine that is robustly displayed on the Class I MHC molecules. We define an MHC genotype to be a set of 3-6 alleles. NetMHCpan4.1 and provides binding predictions between peptides and individual alleles rather than genotypes. To attain credences for whether a peptide is displayed by a genotype, we assume independence between our beliefs that the peptides are displayed by individual alleles, which gives the following:

$$\Pr(display(p, m)) = 1 - \prod_{x \in m} (1 - c_{p,x}) \quad (3)$$

Where  $c_{p,x}$  is the credence for binding between peptide  $p$  and a specific allele  $x$ .

To derive credences for peptide interactions with individual alleles, we input peptide-MHC allele pairs to NetMHCpan4.1. We use the EL rank output, which are values between 0 and 100 that are closer to 0 when binding is more likely and closer to 100 when binding is less likely. We then transform them with a monotonic function to obtain credences for binding between the peptide-MHC pair (see Appendix B for additional details). This transformation was derived using a calibration curve, and was designed so that credences are conservative. To create a calibration curve, we partition the space between the highest and lowest predicted/calibrated values into 100 equally sized bins. The fraction of peptides that are experimentally verified binders are then computed for each bin, producing a curve. A calibration function was then fitted so that after calibrating the predicted value, this procedure produces a curve where the x-axis can be reasonably interpreted as binding credences. See Appendix B for additional details. The calibration curves for the raw predicted values and calibrated values are shown in Figure 1.

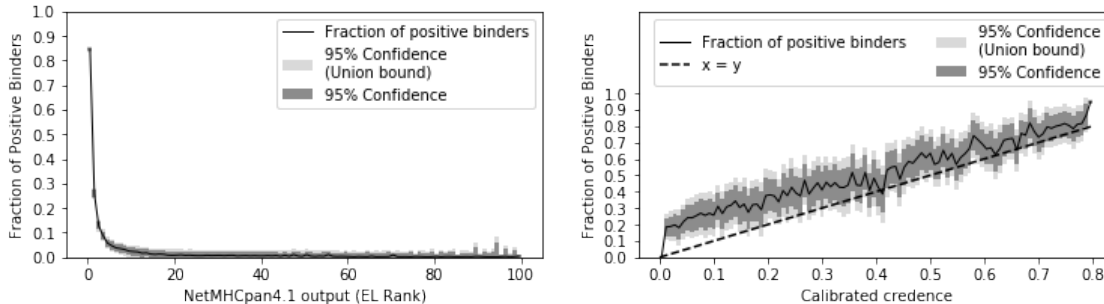


Fig. 1: Each peptide in a test set of 946141 peptides that NetMHCpan4.1 was not trained on was acquired from [12] and was fed into NetMHCpan4.1 to produce predictions (EL rank). The peptides were then binned into 100 disjoint bins of equal size based on their predicted values. For each bin, we calculated the fraction of the peptides that were experimentally observed in binding assays. The 95% confidence interval was computed using Hoeffding’s Inequality[4], such that the probability that a given point lies outside the darker region is at most 5%, while the probability that any part of the curve lies outside the lighter region is at most 5% (derived using the union bound).

## 4 Results

### 4.1 Benchmarking against past vaccine formulation methodologies

We benchmark the diminishing returns vaccine design framework by comparing its vaccine designs for SARS-CoV-2 to designs from the maximum  $n$ -times coverage method that was found to outperform 29 other methods [6]. For the purposes of this benchmark, instead of using credences for peptide-MHC binding as described in Section 3.2, we will use 0-1 credences that mirror the indicator values used in Liu et al. [6]. We used the same set of processed candidate peptides used by Liu et al. [6], which was filtered for peptides with glycosylation, high mutation rates, and cleavage. We also acquired the MHC diplotype frequencies they derived to use as our MHC genotype weights. Finally, we enforce pairwise constraints so that no two peptides in the vaccine formulation can have a Levenshtein distance less than or equal to 3, which mirrors the constraints used by Liu et al. [6]. This guarantees that we will not produce a vaccine formulation that they could not have generated.

For our choice of utility  $U$ , we will use a threshold utility  $U(x) = \min(x, 8)$ . This most closely matches the EvalVax  $n$ -times coverage utility used in Liu et al. [6] since it maximizes the utility of peptides at coverage rates close to the threshold out of all available functions. The threshold utility can be viewed as an instrumental objective to guide the greedy algorithm towards a solution that achieves good multiple coverage.

We evaluate our designs using the EvalVax design objective as laid out in [6]. Note that EvalVax differs from our objective function in that EvalVax allows each peptide to count for multiple hits if they are predicted to interact with multiple MHCs in a given genotype, while our objective only allows each peptide to count for one hit at most. Therefore, the optimization and evaluation objectives differ slightly for our design.

We compare the performance of our design against those from [6] for coverage depths of 1-15. The comparison can be found in Figure 2. Our design is competitive at lower coverage rates, while it performs significantly better at higher coverage rates.

### 4.2 Designing a Sars-CoV2 vaccine using the diminishing returns framework

The diminishing returns framework allows us to consider a variety of utility functions that model the relationship between the number of displayed peptides to vaccine immunogenicity. We opt to use a utility function with parameter  $p$  that models the frequency of system failure under independence:

$$U_p(x) = 1 - (1 - p)^x \quad (4)$$

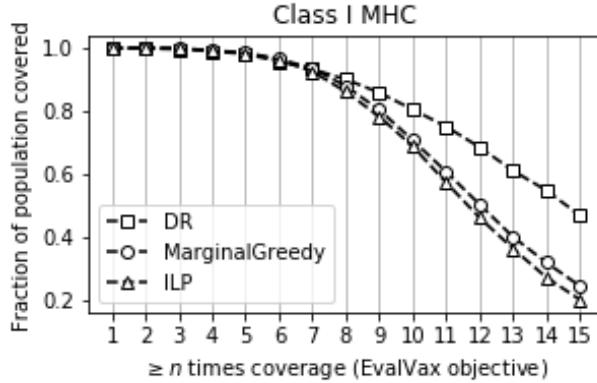


Fig. 2: Comparison of the diminishing returns vaccine formulation against past designs that were optimized against the EvalVax objective function [6]. The EvalVax reported rates of population coverage are given on the y-axis as a function of the desired level of coverage on the x-axis. DR refers to the diminishing returns vaccine formulation, while MarginalGreedy and ILP are the vaccine formulations provided in [6]. Each plotted design contains 19 peptides.

This is a monotonically increasing concave function. To prevent numerical issues, we let  $U_p(x)$  be constant for  $x > \frac{6}{\log_{10}(1-p)}$ . In other words, we stop  $U_p(x)$  from increasing once  $U_p(x)$  is less than  $10^{-6}$  away from 1.

This function has the following probabilistic interpretation: suppose each displayed peptide induces an immunogenic response with probability  $p$ . Then  $U_p(x)$  is the probability that an immune response is induced when there are  $x$  peptides displayed if the probabilities were independent.  $\mathcal{F}_{U_p}(S)$  can then be viewed as the unconditional probability that the vaccine design induces an immunogenic response in some individual selected uniformly at random from the population.

In addition, since the candidate peptide sets were generated using data from February 2021[6], we reduce the credence of observing a peptide-MHC hit to 0 for any peptide absent from the Omicron BA.1 or the Omicron BA.2 variant of SARS-CoV-2. These peptides were generated by translating all open reading frames from representative genomes of Omicron BA.1 (accession number OM873778) and Omicron BA.2 (accession number OW123901) retrieved from the The COVID-19 Data Portal[3].

We generate designs of sizes between 1-100 inclusive optimized against  $\mathcal{F}_{U_{1/5}}$ . We compare the performance of our designs that optimized against  $\mathcal{F}_{U_{1/5}}$  against past designs from [6] on  $\mathcal{F}_{U_{1/3}}$ ,  $\mathcal{F}_{U_{1/5}}$  and  $\mathcal{F}_{U_{1/8}}$  in Figure 3. Our design traces out a trajectory that lies above all other designs for all 3 objectives. We also compare the performance against a set of randomly generated designs. To generate a set of random designs, we sampled peptide sequences randomly from our filtered candidate pool, and added one if it did not violate any pairwise constraints, and if it had some predicted probability of being displayed on some genotype in the population. This was repeated until we attain designs of sizes 1-100 inclusive, and then the overall process was repeated 50 times to produce a total of 5000 designs.

We note that our evaluation model in Figure 3 is based on our credence model and does not incorporate clinical data like the evaluations model adapted from Liu et al. [6] we used in Figure 2. However, Figure 3 does show that given an appropriate objective the optimization procedure will generate good designs relative to that objective, and incorporating clinical data into our credence model is a straightforward question of Bayesian inference.

## 5 Discussion

We have introduced the diminishing returns framework for designing epitope based peptide vaccines. The framework is based on constrained submodular optimization, which permits us to provide performance guarantees despite the NP-hardness of the problem, unlike previous approaches. We also show how we can probabilistically interpret the outputs of machine learning models to allow reasoning with uncertainty within



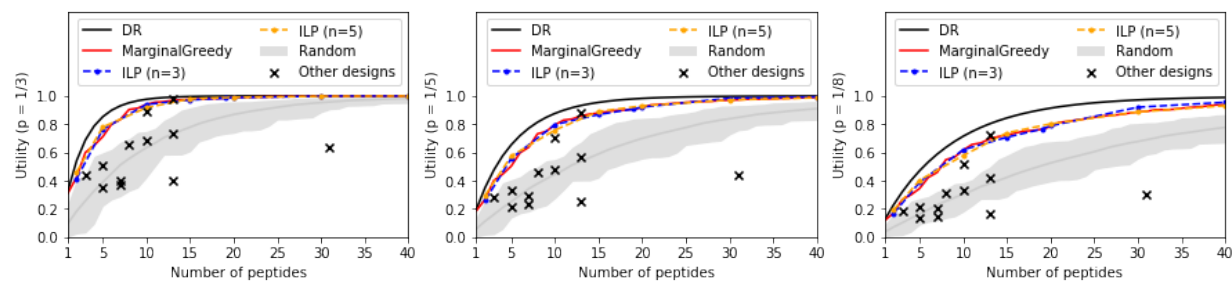


Fig. 3: Comparison of vaccine formulations on the objectives  $\mathcal{F}_{U_{1/3}}$ ,  $\mathcal{F}_{U_{1/5}}$ , and  $\mathcal{F}_{U_{1/8}}$ . The DR line traces out the designs generated by diminishing returns, while the MarginalGreedy and ILP lines are designs from Liu et al. [6]. The performance and sizes of other existing designs are also given, which were used for benchmarking in Liu et al. [6]. The grey area gives the range of values attained by random designs, and the light grey line gives the mean of the utilities of the random designs at each size.

the framework. Finally, we demonstrated that this framework achieves superior performance against past vaccine designs on the SARS-CoV-2 vaccine design task, and achieves comparable performance even when evaluated against previous objectives.

Our approach is highly scalable, allowing us to optimize over potentially millions of candidate peptides for a single vaccine. The ability to reason with uncertainty also gives us a much richer language for expressing the properties of a peptide: for instance, instead of filtering out peptides prone to mutation, we can consider the probability of sequence drift. These factors allow us to consider a far wider range of peptide vaccine design tasks, which we plan to use in the future.

## Data availability

Code and processed data are available at <https://github.com/gifford-lab/DiminishingReturns>.

## References

- [1] Travers Ching, Daniel S Himmelstein, Brett K Beaulieu-Jones, Alexandr A Kalinin, Brian T Do, Gregory P Way, Enrico Ferrero, Paul-Michael Agapow, Michael Zietz, Michael M Hoffman, et al. Opportunities and obstacles for deep learning in biology and medicine. *Journal of The Royal Society Interface*, 15(141):20170387, 2018.
- [2] Uriel Feige. A threshold of  $\ln n$  for approximating set cover. *Journal of the ACM (JACM)*, 45(4):634–652, 1998.
- [3] Peter W Harrison, Rodrigo Lopez, Nadim Rahman, Stefan Gutnick Allen, Raheela Aslam, Nicola Buso, Carla Cummins, Yasmin Fathy, Eloy Felix, Mihai Glont, et al. The covid-19 data portal: accelerating sars-cov-2 and covid-19 research through rapid open access data sharing. *Nucleic acids research*, 49(W1):W619–W623, 2021.
- [4] Wassily Hoeffding. Probability inequalities for sums of bounded random variables. In *The collected works of Wassily Hoeffding*, pages 409–426. Springer, 1994.
- [5] Weidang Li, Medha D Joshi, Smita Singhania, Kyle H Ramsey, and Ashlesh K Murthy. Peptide vaccine: progress and challenges. *Vaccines*, 2(3):515–536, 2014.
- [6] Ge Liu, Alexander Dimitrakakis, Brandon Carter, and David Gifford. Maximum n-times coverage for vaccine design, 2021. URL <https://arxiv.org/abs/2101.10902>.
- [7] Ryan J Malonis, Jonathan R Lai, and Olivia Vergnolle. Peptide-based vaccines: current progress and future challenges. *Chemical reviews*, 120(6):3210–3229, 2019.
- [8] Leonard Moise, Andres Gutierrez, Farzana Kibria, Rebecca Martin, Ryan Tassone, Rui Liu, Frances Terry, Bill Martin, and Anne S De Groot. ivax: An integrated toolkit for the selection and optimization of antigens and the design of epitope-driven vaccines. *Human vaccines & immunotherapeutics*, 11(9):2312–2321, 2015.

- [9] George L Nemhauser, Laurence A Wolsey, and Marshall L Fisher. An analysis of approximations for maximizing submodular set functions—i. *Mathematical programming*, 14(1):265–294, 1978.
- [10] Patricio Oyarzun and B Kobe. Computer-aided design of t-cell epitope-based vaccines: addressing population coverage. *International journal of immunogenetics*, 42(5):313–321, 2015.
- [11] Prasad Raghavendra and David Steurer. Graph expansion and the unique games conjecture. In *Proceedings of the forty-second ACM symposium on Theory of computing*, pages 755–764, 2010.
- [12] Birkir Reynisson, Bruno Alvarez, Sinu Paul, Bjoern Peters, and Morten Nielsen. Netmhciipan-4.1 and netmhciipan-4.0: improved predictions of mhc antigen presentation by concurrent motif deconvolution and integration of ms mhc eluted ligand data. *Nucleic acids research*, 48(W1):W449–W454, 2020.
- [13] Muhammad Saqib Sohail, Syed Faraz Ahmed, Ahmed Abdul Quadeer, and Matthew R McKay. In silico t cell epitope identification for sars-cov-2: Progress and perspectives. *Advanced drug delivery reviews*, 171:29–47, 2021.
- [14] Anita J Zaitouna, Amanpreet Kaur, and Malini Raghavan. Variations in mhc class i antigen presentation and immunopeptidome selection pathways. *F1000Research*, 9, 2020.
- [15] David Zuckerman. Linear degree extractors and the inapproximability of max clique and chromatic number. In *Proceedings of the thirty-eighth annual ACM symposium on Theory of computing*, pages 681–690, 2006.

# Appendices



## A Proofs

### A.1 Proof of Theorem 1

For reference, we state the definition of  $\text{GAP-SMALL-SET EXPANSION}(\eta)$  adapted from [11]:

**Definition 2.** *Given a  $d$ -regular graph  $G = (V, E)$  and some integer  $k$ , determine which of the following is the case:*

1. *There exists  $S \subseteq V$  with  $|S| = k$  such that the number of edges leaving  $S$  is less than  $dk\eta$ .*
2. *For all  $S \subseteq V$  where  $|S| = k$ , the number of edges leaving  $S$  is more than  $dk(1 - \eta)$ .*

This is a promise problem: if neither is true then we are free to output whatever we want.

Suppose that there exists a polynomial time algorithm that approximates  $n$ -times coverage to an approximation ratio of  $\epsilon > 0$  (i.e. if  $OPT$  is the value of the true solution, the solution returned by the algorithm attains value  $\epsilon OPT$ ).

Then there exists an  $\eta \in (0, 0.5)$  such that we can solve  $\text{GAP-SMALL-SET EXPANSION}(\eta)$ : given an input  $d$ -regular graph, let each vertex represent a peptide, and let each edge represent a genotype. A peptide is displayed by a genotype if and only if the vertex represented by that peptide is incident to the edge represented by that genotype. We then compute an approximation for max 2-times coverage using our algorithm with cardinality constraint  $k$ .

Let  $\hat{S}$  be the value of the solution returned by the algorithm, and let  $S^*$  be the value of the optimal solution. Let  $\hat{E}$  be the number of genotypes covered by  $\hat{S}$  and let  $E^*$  be the number of genotypes covered by  $S^*$ .

Let  $f(x) = dk - 2x$ . Since each vertex has degree  $k$ , and  $\hat{E}$  and  $E^*$  are the number of edges that have both endpoints in  $\hat{S}$  and  $S^*$  respectively,  $f(\hat{E})$  and  $f(E^*)$  are the number of edges that leave  $\hat{S}$  and  $S^*$  respectively.

Let  $p$  be some sufficiently large value that is greater than 0 such that  $\epsilon(1 - \epsilon^p) > \epsilon^p$  and such that  $\epsilon^p < 0.5$ . Output case 1 if  $f(\hat{E}) < dk(1 - \epsilon^p)$ , and output case 2 otherwise.

This procedure completes in polynomial time, and we claim that this correctly solves  $\text{GAP-SMALL-SET EXPANSION}(\epsilon^p)$ . To verify this, suppose that we are in case 1. We then have:

$$f(E^*) < \epsilon^p \tag{5}$$

$$dk(1 - \epsilon^p) < 2E^* \tag{6}$$

Since  $\hat{S}$  attains an approximation ratio of  $\epsilon$ , we have:

$$f(\hat{E}) \leq f(\epsilon E^*) \tag{7}$$

$$< f(\epsilon dk(1 - \epsilon^p)) \tag{8}$$

$$= dk(1 - \epsilon(1 - \epsilon^p)) \tag{9}$$

$$< dk(1 - \epsilon^p) \tag{10}$$

The last line follows since we defined  $p$  to be large enough for that to hold. Since  $f(\hat{E}) < dk(1 - \epsilon^p)$ , the algorithm indeed outputs case 1.

Suppose instead that we are in case 2. But then  $f(\hat{E}) > dk(1 - \epsilon^p)$  because all sets of size  $k$  have more than  $dk(1 - \epsilon^p)$  edges leaving it. Therefore, the algorithm correctly outputs case 2.

Therefore, this procedure decides  $\text{GAP-SMALL-SET EXPANSION}(\epsilon^p)$  in polynomial time.

### A.2 Proof of Theorem 2

Let  $S \subseteq T \subsetneq \mathcal{P}$ , and let  $e \in U \setminus T$ . Let  $S' = S \cup \{e\}$  and let  $T' = T \cup \{e\}$ . It suffices to show that  $\mathcal{F}_U(S') - \mathcal{F}_U(S) \geq \mathcal{F}_U(T') - \mathcal{F}_U(T)$ . We have the following:

$$\mathcal{F}_U(S') - \mathcal{F}_U(S) = \sum_{m \in \mathcal{M}} w(m) \mathbb{E}[U(\sum_{p \in S'} \mathbb{1}_{display(p,m)}) - U(\sum_{p \in S} \mathbb{1}_{display(p,m)})] \quad (11)$$

$$= \sum_{m \in \mathcal{M}} w(m) \sum_{u \in \mathcal{U}} \Pr(u) (U(H(S', u)) - U(H(S, u))) \quad (12)$$

Where  $\mathcal{U}$  denotes the set of all possible outcomes (i.e. all possible truth assignments to the predicates  $display(p, m)$  for all  $p \in \mathcal{P}$  and  $m \in \mathcal{M}$ ), and  $H(S, u)$  denotes the number of hits found in set  $S$  under outcome  $u$ .  $\Pr(u)$  denotes the probability assigned to outcome  $u$ .

Since  $S \subseteq T$ , it must be the case that  $H(S, u) \leq H(T, u)$  for any outcome  $u \in \mathcal{U}$ . Since  $e$  is either a hit or not a hit under outcome  $u$ ,  $H(S', u) - H(S, u) = H(T', u) - H(T, u) = H(\{e\}, u)$  for any outcome  $u \in \mathcal{U}$ .

When these two conditions are paired with the observation that  $U$  is concave, we have:

$$\mathcal{F}_U(S') - \mathcal{F}_U(S) = \sum_{m \in \mathcal{M}} w(m) \sum_{u \in \mathcal{U}} \Pr(u) (U(H(S', u)) - U(H(S, u))) \quad (13)$$

$$\geq \sum_{m \in \mathcal{M}} w(m) \sum_{u \in \mathcal{U}} \Pr(u) (U(H(T', u)) - U(H(T, u))) \quad (14)$$

$$= \mathcal{F}_U(T') - \mathcal{F}_U(T) \quad (15)$$

Which then implies that  $\mathcal{F}_U$  is submodular.

### A.3 Proof of Theorem 3

If  $\Delta(\mathcal{G}) = 0$ , then there are not constrains, and it is well established that the greedy approach indeed attains an approximation ratio of  $(1 - e^{-1})[9]$ .

Let  $e_1, e_2, \dots, e_a$  be the elements chosen by Algorithm 1, in that order. Let  $o_1, o_2, \dots, o_b$  be the elements of  $S_2^* \setminus \hat{S}$ .

Pair an  $e_i$  an  $o_j$  if  $e_i$  shares an edge with  $o_j$ . If a single  $o_j$  shares edges with multiple  $e_i$ , choose the pair randomly. A single  $e_i$  cannot share edges with more than one  $o_j$ , since otherwise that would imply that there exists a path of length two between those two  $o_j$  that passes through the  $e_i$ .

Suppose some  $o_j$  are left over. We then pair them up randomly with the remaining  $e_i$ . If there are unpaired elements, it must be the  $e_i$ , since otherwise the unpaired  $o_j$  would have been added to the greedy solution.

Now consider the trajectory of adding elements to a solution in the order  $e_1, e_2, \dots, e_a, o_1, o_2, \dots, o_b$ . By monotonicity, this must attain a value at least as great as  $S_2^*$ .

Suppose  $e_i$  is paired with  $o_j$ . Then the marginal improvement of taking  $e_i$  must have been better than the marginal improvement of taking  $o_j$ , since otherwise  $o_j$  would have been chosen instead of  $e_i$ . Therefore, the score attained by  $e_1, e_2, \dots, e_a, o_1, o_2, \dots, o_b$  cannot be more than 2 times larger than the score attained by  $e_1, e_2, \dots, e_a$ . But since the value attained by  $S_2^*$  can be no greater than  $e_1, e_2, \dots, e_a, o_1, o_2, \dots, o_b$ , it must be the case that the value attained by  $S_2^*$  is no more than 2 times larger than the value attained by the greedy solution.

Similarly, let  $q_1, q_2, \dots, q_b$  be the elements of  $S^* \setminus \hat{S}$ . We similarly associate  $e^i$  with  $q_j$  if they share an edge, and if a  $q_j$  shares edges with multiple  $e_i$  the association is chosen arbitrarily. Note that no  $e_i$  can be associated with more than  $\Delta(\mathcal{G})$   $q_j$ .

We associate the remaining  $q_j$  with  $p_i$  such that no  $p_i$  is associated with more than  $\Delta(\mathcal{G})$   $q_j$ . If there are leftovers they must belong to  $\hat{S}$  because otherwise they would have been included in the greedy solution.

Now consider the trajectory of adding elements to a solution in the order  $e_1, e_2, \dots, e_a, q_1, q_2, \dots, q_b$ . By monotonicity, this must attain a value at least as great as  $S^*$ .

Suppose  $e_i$  is associated with  $q_j$ . Then the marginal improvement of taking  $e_i$  must have been better than the marginal improvement of taking  $q_j$ , since otherwise  $q_j$  would have been chosen instead of  $e_i$ . Since each  $e_i$  can be associated with up to  $\Delta(\mathcal{G})$   $q_i$ , the score attained by  $e_1, e_2, \dots, e_a, q_1, q_2, \dots, q_b$  can be no larger than  $\Delta(\mathcal{G}) + 1$  times the value attained by  $\hat{S}$ . But then that means  $S^*$  does not attain a value that is more than  $\Delta(\mathcal{G}) + 1$  times the value of the greedy solution.

#### A.4 Proof of Theorem 4

We restate the two approximation guarantees that cannot be given if  $P \neq NP$ :

1.  $\mathcal{F}_U(\hat{S}) \geq \mathcal{F}_U(S_2^*)(1 - \frac{1}{e} + \epsilon)$
2.  $\mathcal{F}_U(\hat{S}) \geq (\frac{\mathcal{F}_U(S^*)}{1 + \Delta(\mathcal{G})})^{(1-\epsilon)}$

To establish the first inapproximability result, we can encode an instance of max  $k$ -cover in our optimization problem: let each genotype represent a member of the ground set and let each peptide represent an element of the set system. We let the genotype display a peptide with probability 1 if the element represented by the peptide is contained in the set represented by the genotype, and with probability 0 otherwise. Define the concave utility function as  $U(x) = \min(x, 1)$ , and let  $\mathcal{G}$  be a set of unconnected vertices, so  $\mathcal{F}_U(S^*) = \mathcal{F}_U(S_2^*)$ . If each genotype is given weight 1, then  $\mathcal{F}_U(S)$  gives the number of elements covered by  $S$ . The first inapproximability result then follows from the inapproximability of max  $k$ -cover to a ratio of  $(1 - \frac{1}{e} + \epsilon)$  for any  $\epsilon > 0$ [2].

To establish the second inapproximability result, we can encode an instance of independent set in our optimization problem: let each peptide represent a vertex, and for each peptide introduce a genotype that displays that peptide with probability 1 and displays all other peptides with probability 0. Define the concave utility function as  $U(x) = \min(x, 1)$ . If each genotype is given weight 1, then  $\mathcal{F}_U(S)$  gives the number of elements contained in  $S$ . If we set  $\mathcal{G}$  to be the instance of independent set we wish to encode, then  $\mathcal{F}_U(S^*)$  is the size of the largest independent set. The second inapproximability result then follows from the fact that independent set cannot be approximated to a ratio of  $|\mathcal{G}_V|^{1-\epsilon}$  for any  $\epsilon > 0$ [15], and from the fact that  $1 + \Delta(\mathcal{G}) \leq |\mathcal{G}_V|$ .

## B Calibration

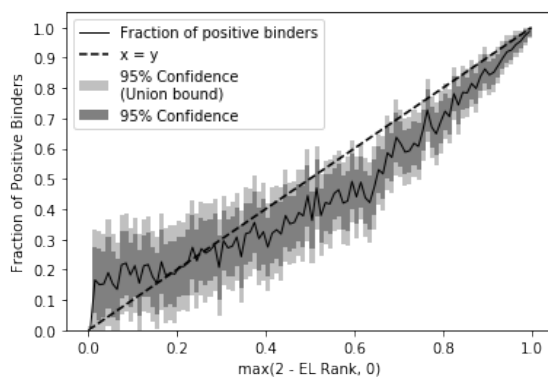
We calibrate NetMHCpan4.1 using a validation dataset of 946141 samples derived from Single-Allele Eluted Ligands datasets that were used for benchmarking NetMHCpan4.1 and did not contain samples used to train it [12]. To create a calibration curve, we partition the space between the highest and lowest predicted/calibrated values into 100 equally sized bins. The fraction of peptides that are experimentally verified binders within the validation datasets are then computed for each bin, producing a curve.

NetMHCpan4.1 outputs EL %Rank as one score for determining whether a peptide sequence interacts with an MHC [12]. The EL %Rank score ranges from 0 to 100, where values closer to 0 indicate a higher chance of interaction and values closer to 100 indicate a lower chance of interaction. We can see in Figure 1 that for most values of EL %Rank there is almost no observed interaction. NetMHCpan4.1 does not consider anything with a predicted score above 2 to be a binder by default, so our first attempt is to set binding credences to 0 for all scores above 2 and linearly interpolate between a credence of 0 and 1 for scores between 2 and 0. The results can be seen in Figure 4a.

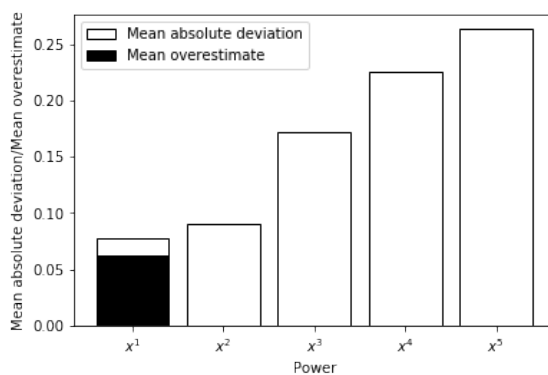
We note that there is a clear monotonic trend. The curve is slightly concave, so we adjust it by feeding the score through a monomial. Figure 4 shows the mean absolute deviation (MAD) between the calibration curve and the line  $y = x$ . To compute the MAD, we take for each bin the absolute value of the difference between the midpoint of the bin and the fraction of peptides that are verified binders, and then take the average over the bins. We also compute the mean overestimate, which we compute by taking the midpoint of each bin, subtracting off the fraction of peptides that are verified binders in that bin, setting the value to 0 if it is below 0, and then taking the average over the bins. This mean overestimate quantifies how much of the curve lies below  $x = y$ , and can be thought of as a measure of unsoundness.

The MAD and mean overestimates are given in Figure 4b for various monomials. Although the identity function  $f(x) = x^1$  gives the best MAD,  $f(x) = x^2$  gives a similar MAD while having a much lower mean overestimate. Therefore, we choose to use  $x^2$  since it provides much sounder credences while providing a similar MAD.

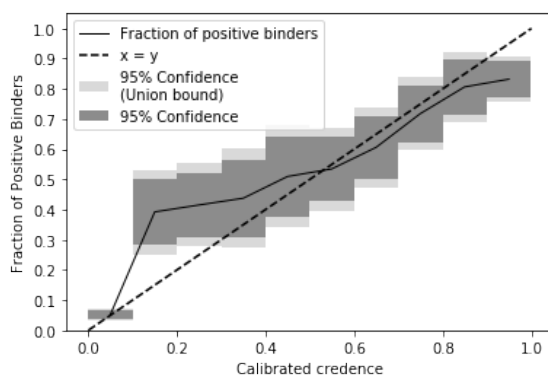
We validate our calibrated curve with a separate validation dataset of 1581 epitopes also used for validating NetMHCpan4.1 [12]. This dataset did not provide negative samples in the same way as the dataset used to calibrate the curve, so decoys were generated by producing 5 random permutations of the sequences of each epitope. A calibration curve with 10 bins was created using calibrated predictions for the resulting



(a) Calibration curve where the calibrated values are linearly interpolated from 0 to 1 for EL %Rank values between 2 and 0. EL %Rank values above 2 are assigned a value of 0.



(b) Mean absolute deviation (MAD) and mean overestimates for the monomials  $x$ ,  $x^2$ ,  $x^3$ ,  $x^4$ , and  $x^5$ . The portion of the MAD that is accounted for by the mean overestimate is filled in black.



(c) Calibration curve on a separate dataset of 9486 samples, where calibrated credences are obtained from EL %Rank scores via  $\frac{\max(2 - \text{EL \%Rank}, 0)^2}{4}$ .

Fig. 4: Calibration of EL %Rank scores



dataset of 9486 samples, which is given in Figure 4c. While the curve was close to  $x = y$ , we note that the curve tapers off at 0.8. Therefore, we cap our maximum credence at 0.8.

The final transformation from EL %Rank scores to credences is the following:

$$\text{Credence} = \min\left(\frac{\max(2 - \text{EL \%Rank}, 0)^2}{4}, 0.8\right) \quad (16)$$

## C Implementation details

### C.1 Computing $\mathcal{F}_U$

To compute  $\mathcal{F}_U(S)$  in time  $\mathcal{O}(|\mathcal{M}||S|^2)$ , it suffices to calculate  $\mathbb{E}[U(\sum_{p \in S} \mathbb{1}_{\text{display}(p,m)})]$  in time  $\mathcal{O}(|S|^2)$  for each  $m \in \mathcal{M}$  since we can then add up all the values.

To calculate  $\mathbb{E}[U(\sum_{p \in S} \mathbb{1}_{\text{display}(p,m)})]$  in time  $\mathcal{O}(|S|^2)$ , we use iterated convolutions. We store a zero indexed list  $D$  of size  $|S| + 1$  initialized such that  $D_i = 0$  except for  $i = 0$ , where we have  $D_0 = 1$ . Then for each  $p \in S$ , we loop in reverse order from  $i = |S|$  to  $i = 0$  and update the list by setting  $D_i$  to  $(1 - x)D_i + (x)D_{i-1}$ , where  $x$  is the credence that  $p$  is displayed by  $m$ .  $D_0$  is set to  $(x)D_0$ . The result is a convolution of a distribution with probability mass function  $D$  a Bernoulli random variable whose chance of success is  $x$ . In other words, after each iteration of the loop the value of  $D_i$  represents the probability of attaining  $i$  hits from a vaccine given the peptides that have already been looped over. Performing this loop for all members of  $S$  then gives the probability distribution for  $\sum_{p \in S} \mathbb{1}_{\text{display}(p,m)}$  if all random variables in the sum are independent. We can then take the expectation by using the identity  $\mathbb{E}[f(Y)] = \sum_y f(y)\Pr(Y = y)$ . Each loop runs in time  $\mathcal{O}(|S|)$ ,  $\mathcal{O}(|S|)$  loops need to be run, so computing the distribution takes time  $\mathcal{O}(|S|^2)$  overall. If the utility function is provided in some data structure that allows random access (e.g. an array), then the expectation can be computed in time  $\mathcal{O}(|S|)$ . Thus,  $\mathbb{E}[U(\sum_{p \in S} \mathbb{1}_{\text{display}(p,m)})]$  can be calculated in time  $\mathcal{O}(|S|^2)$ , which gives an overall runtime of  $\mathcal{O}(|\mathcal{M}||S|^2)$  for calculating  $\mathcal{F}_U(S)$ .

### C.2 Computing the marginal improvement

Let  $S$  be fixed, and suppose  $S' = S \cup \{e\}$  for some  $e \in \mathcal{P}$ . Then we can calculate  $\mathcal{F}_U(S') - \mathcal{F}_U(S)$  in time  $\mathcal{O}(|\mathcal{M}||S|)$  instead if we store the distribution of  $\sum_{p \in S} \mathbb{1}_{\text{display}(p,m)}$  for each  $m \in \mathcal{M}$ . This is because we only need to convolve a single Bernoulli random variable over the distribution of  $\sum_{p \in S} \mathbb{1}_{\text{display}(p,m)}$  to get the distribution of  $\sum_{p \in S'} \mathbb{1}_{\text{display}(p,m)}$ . This then allows us to calculate the expectation in time  $\mathcal{O}(|S|)$ , which then gives an overall runtime of  $\mathcal{O}(|\mathcal{M}||S|)$  for calculating the marginal improvement.

At the end of each greedy step, we can update the distributions of  $\sum_{p \in S} \mathbb{1}_{\text{display}(p,m)}$  to  $\sum_{p \in S'} \mathbb{1}_{\text{display}(p,m)}$  for all  $m \in \mathcal{M}$  in time  $\mathcal{O}(|\mathcal{M}||S|)$  by performing a single convolution between the distribution and a Bernoulli random variable.

### C.3 Vectorization

The calculation of the marginal differences can be vectorized: let  $D'$  be the probability mass function of  $\sum_{p \in S'} \mathbb{1}_{\text{display}(p,m)}$  and let  $D$  be the probability mass function of  $\sum_{p \in S} \mathbb{1}_{\text{display}(p,m)}$ . Let  $x$  be the credence that the element in  $S' \setminus S$  is displayed on  $m$ . Let  $D$  and  $D'$  be represented by vectors where  $D_i$  is the probability that the random variable distributed with probability mass function  $D$  takes on value  $i$ , and likewise for  $D'$ . Let  $U$  be a vector representing the utility function, where  $U_i = U(i)$ . Then the expected value of  $U(Y)$  is  $U \cdot D$  if  $Y$  is distributed with probability mass function  $D$  (likewise for  $D'$ ).

If  $Z$  is a vector, let  $Sh(Z)$  denote a shift operation where  $Sh(Z)_i = Z_{i-1}$  and  $Sh(Z)_0 = 0$ . Let  $Sh^{-1}(Z)$  be the reverse operation where  $Sh(Z)_i = Z_{i+1}$  and  $Sh(Z)_n = 0$  if  $n$  is the size of  $Z$ . If we ensure that the entry at the last index of  $D$  is 0 such that  $Z \cdot D = Sh(Z) \cdot Sh(D)$  and  $Sh^{-1}(Sh(D)) = D$ , then the marginal difference is:

$$\mathbb{E}[U(\sum_{p \in S'} \mathbb{1}_{\text{display}(p,m)})] - \mathbb{E}[U(\sum_{p \in S} \mathbb{1}_{\text{display}(p,m)})] = U \cdot D' - U \cdot D \quad (17)$$

This can be rearranged as the following:

$$U \cdot D' - Sh(U) \cdot Sh(D) = U \cdot ((x)Sh(D) + (1-x)D) - Sh(U) \cdot Sh(D) \quad (18)$$

$$= U \cdot (x)Sh(D) - (x)Sh(U) \cdot Sh(D) \quad (19)$$

$$= (x)(U - Sh(U)) \cdot (sh(D)) \quad (20)$$

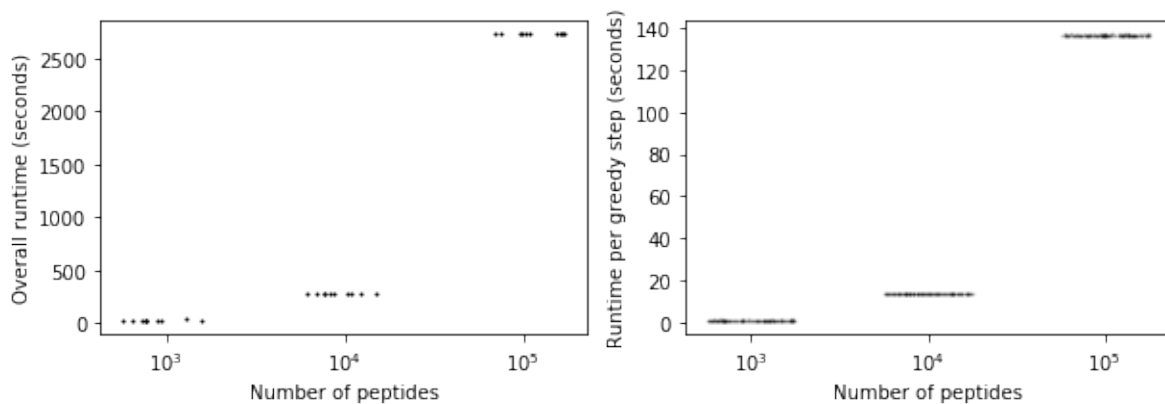
$$= (x)(Sh^{-1}(U) - U) \cdot D \quad (21)$$

Therefore, if we precompute and vectorize  $(Sh^{-1}(U) - U)$ , the marginal difference is simply a scaled dot product. This is a vector operation. We can then further tensor over  $\mathcal{M}$  and  $\mathcal{P}$  to parallelize most of the operations.

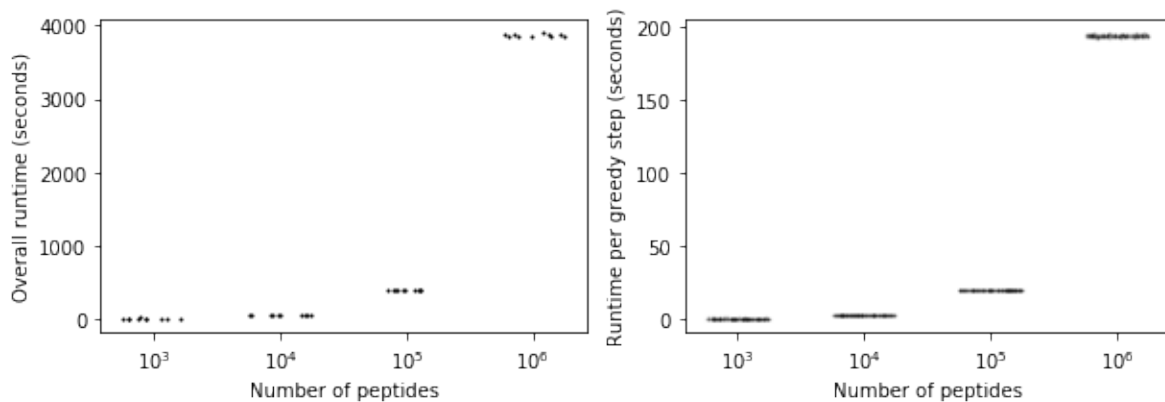
#### C.4 Runtime

We benchmarked the runtime of Algorithm 1 by generating vaccine designs of size 20 using synthetic datasets where binding credences are drawn uniformly and independently between 0 and 1, with  $|\mathcal{M}| = 10^6$  and varying sizes of  $|\mathcal{P}|$ . 10 runs were executed for each  $|\mathcal{P}|$ . We ran the benchmarks both parallelized over 8 Titan RTX GPUs and on a single Titan RTX GPU. The results are given in Figure 5A and 5B.

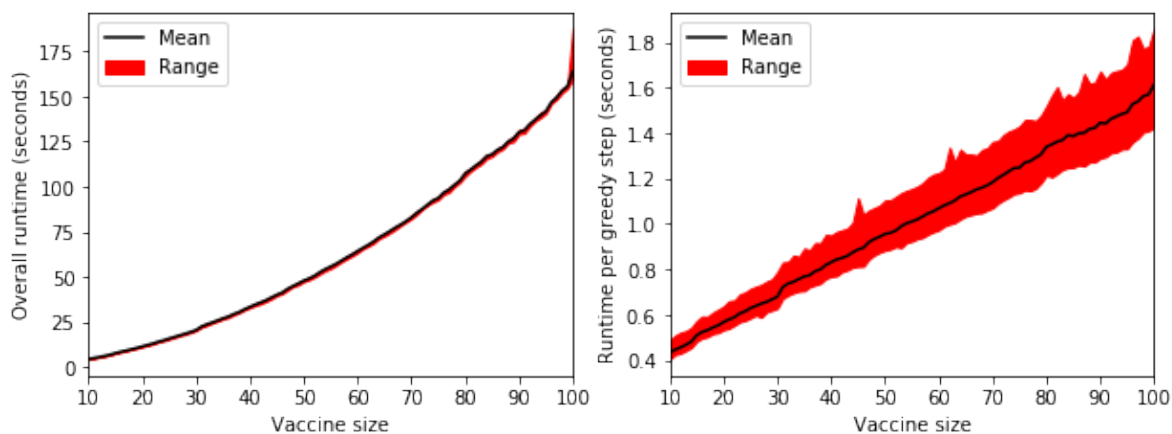
Furthermore, we fixed  $|\mathcal{P}|$  to  $10^3$ , and generated vaccine designs of size between 10 and 100 inclusive. The runtimes are given in Figure 5C.



(a) Overall runtimes of Algorithm 1 on one Titan RTX GPU are provided in strip plots on the left panel. Each box is generated from 10 executions. Overall runtimes for each greedy iteration on one Titan RTX GPU are provided on the right panel, where is box is generated from 200 runtimes (20 iterations for 10 runs).



(b) Overall runtimes of Algorithm 1 on 8 Titan RTX GPUs are provided in strip plots on the left panel. Each box is generated from 10 executions. Overall runtimes for each greedy iteration on 8 Titan RTX GPUs are provided on the right panel, where is box is generated from 200 runtimes (20 iterations for 10 runs).



(c) Average runtimes over 10 executions of Algorithm 1 on 8 Titan RTX GPUs are plotted in the left panel, parameterized by the size of the vaccine design. The range of runtimes are also given. Average runtimes for each greedy iteration on 8 Titan RTX GPUs are provided on the right panel, along with the observed ranges.

Fig. 5: Runtime benchmarks

## References

- [2] Uriel Feige. A threshold of  $\ln n$  for approximating set cover. *Journal of the ACM (JACM)*, 45(4): 634–652, 1998.
- [9] George L Nemhauser, Laurence A Wolsey, and Marshall L Fisher. An analysis of approximations for maximizing submodular set functions—i. *Mathematical programming*, 14(1):265–294, 1978.
- [11] Prasad Raghavendra and David Steurer. Graph expansion and the unique games conjecture. In *Proceedings of the forty-second ACM symposium on Theory of computing*, pages 755–764, 2010.
- [12] Birkir Reynisson, Bruno Alvarez, Sinu Paul, Bjoern Peters, and Morten Nielsen. Netmhciipan-4.1 and netmhciipan-4.0: improved predictions of mhc antigen presentation by concurrent motif deconvolution and integration of ms mhc eluted ligand data. *Nucleic acids research*, 48(W1):W449–W454, 2020.
- [15] David Zuckerman. Linear degree extractors and the inapproximability of max clique and chromatic number. In *Proceedings of the thirty-eighth annual ACM symposium on Theory of computing*, pages 681–690, 2006.